CHALMERS

Microwave radiometry:
the impact on observed brightness temperature due to water droplets on the feed system

Technical Report

JONAS WAHLBOM
wahlbom@chalmers.se

Department of Earth and Space Sciences
CHALMERS UNIVERSITY OF TECHNOLOGY
Gothenburg, Sweden, 2012
Report No. 9

Abstract

The water vapour radiometer Astrid at the Onsala Space Observatory measures the downward radiation from atmospheric water vapour. During and after a rainfall droplets stay on the reflector and on the transmission window and cause an increase in the measured antenna brightness temperature, T_A. Four different cases were investigated in this report. Case 1, when the reflector was sprayed with droplets resulted in a 4 K increase in T_A. In Case 2, where the transmission window was sprayed with droplets, a 34 K increase in T_A was found. In Case 3 both of them was sprayed with droplets which resulted in a 74 K increase in T_A. In Case 4 droplets were placed in a grid on the reflector which resulted in a 13 K increase in T_A. As a reference the sky brightness temperature during the measurements was independently monitored by a second radiometer at the site. It shows stable results in all four cases. The weather conditions during the first experiment day (Case 1–3), July 26, were sunny and clear with a ground temperature that ranged from 17 °C to 19 °C, a relative humidity of 74 % and an air pressure of 1015 hPa. On the second day (Case 4), August 31, the weather was partly cloudy with a ground temperature at 17 °C, relative humidity of 76 % and air pressure at 1011 hPa.

Contents

1. Introduction

During and after a rainfall droplets stay on the reflector and the transmission window of the Water Vapour Radiometer (WVR). Figure 1 depicts the transmission window after a heavy rainfall on July 31, 2012. This affects the measured sky brightness temperature. A theoretical as well as an experimental background were published by (Jacobson et al., 1986).

This experiment aims to quantify the effect and the time it takes from the rainfall ends until the antenna brightness temperatures are not significantly affected. The Astrid WVR is a dual channel radiometer and normally measures the thermal emission from the atmosphere at a 1 GHz wide frequency band around 21.0 GHz and 31.4 GHz (Elgered and Jarlemark., 1998). The experiments presented in this report were all carried out using the 21.0 GHz channel only and all measurements were only made in the zenith direction with an antenna full width half maximum beam width of 6°. As a reference, time series from a second radiometer are used (Stoew et al., 2000).

Figure 1: The Astrid 21 GHz window just after a heavy rain shower on July 31, 2012.

1.1. Theory

1.1.1. Radiometer observations

The output from Astrid is a voltage proportional to the antenna temperature, T_A, and the system noise temperature T_{sys}. Multiplied with a conversion factor G. The antenna temperature comprise the contributions from the thermal emission from the atmosphere, the cosmic background noise, the emission from rain and water drops on the WVR feed system, and ground noise pick-up. The thermal emission from the atmosphere is a combination of the emissions from water vapour, liquid water and oxygen hereinafter referred to as T_{sky}. The ground noise can be ignored for elevation angels used in this experiment. However, an excess ground noise may be reflected into the antenna when drops are present on the feed system. In this work we define also such a contribution to be included in the drop brightness temperature. The relation between the antenna temperature and the output voltage is given by

$$V_A = (T_A + T_{sys})G^{-1} \tag{1}$$

T_{sys} can be eliminated by using a warm reference load, T_{warm}, as

$$\begin{aligned} V_A - V_{warm} &= (T_A + T_{sys})G^{-1} - (T_{warm} + T_{sys})G^{-1} \\ &= (T_A - T_{warm})G^{-1} \end{aligned} \tag{2}$$

The raw output data are saved in a log file as

$$\begin{aligned} V_{saved} &= |V_A - V_{warm}| \\ &= |(T_A - T_{warm})G^{-1}| \end{aligned} \tag{3}$$

Since T_{warm} and T_{hot} both are continuously monitored the gain G can be calculated from

$$\begin{aligned} V_{hot} - V_{warm} &= (T_{warm} - T_{hot} + \Delta \mathrm{T}_{hot})G^{-1} \\ G &= (T_{warm} - T_{hot} + \Delta \mathrm{T}_{hot})\left(\frac{1}{V_{hot} - V_{warm}}\right) \end{aligned} \tag{4}$$

According to Equation (2) the antenna temperature is

$$T_A = (V_A - V_{warm})G + T_{warm} \tag{5}$$

1.1.2. Evaporation and time constant

The area of the reflector is $A = \pi r^2$. If a drop is modeled as a rectangular box with volume $V_d = A_d h$ m^3 a group of N drops will cover a part of the reflector area given by

$$A_d = \sum_{i=1}^{N} \pi r_i^2 \tag{6}$$

and as they evaporate the covered area decrease with time as

$$A_{covered}(t) = \pi(r(t_0)^2 - |r(t_0)^2 - r(t)^2)|) \tag{7}$$

It is reasonable to assume that when the droplets evaporate the area decrease as a second order polynomial. There is an additional contribution to the antenna brightness temperature, T_A, from these droplets. At the same time they reflect incoming radiation in other directions then the receiving antenna which decrease the contribution from T_{sky}. A time constant τ is defined as the time it takes the water to evaporate from 90 % to 10 % of its maximum contribution in T_A.

1.2. Randomly selected examples

Data from two days in July, one with clouds and rain the other with clear skies, are compared to give a feeling for the radiometer output. The ZWD from GNSS measurements together with the ZWD from Astrid and Konrad on a sunny day, July 25 2012, are shown in Figure 2a and the equivalent output from a rainy day, July 12 2012, in Figure 2b. Rain is indicated by the rain-sensors at the site.

The ZWD from Astrid is in this case calculated only using the 21 GHz channel constantly measuring in the zenith direction whereas Konrad use a dual channel setup measuring at 21.6 GHz and 31.6 GHz in a scanning pattern covering most of the sky. The measurements are mapped to zenith with a mapping function $(1/\sin(\epsilon))$. At periods with rain the ZWD increase rapidly as the rain increase the measured antenna temperature and the samples are eventually treated as outliers by the radiometer software. The GPS measurements are not affected by rain since the observed variable (primarily the phase delay) is almost independent on liquid water drops.

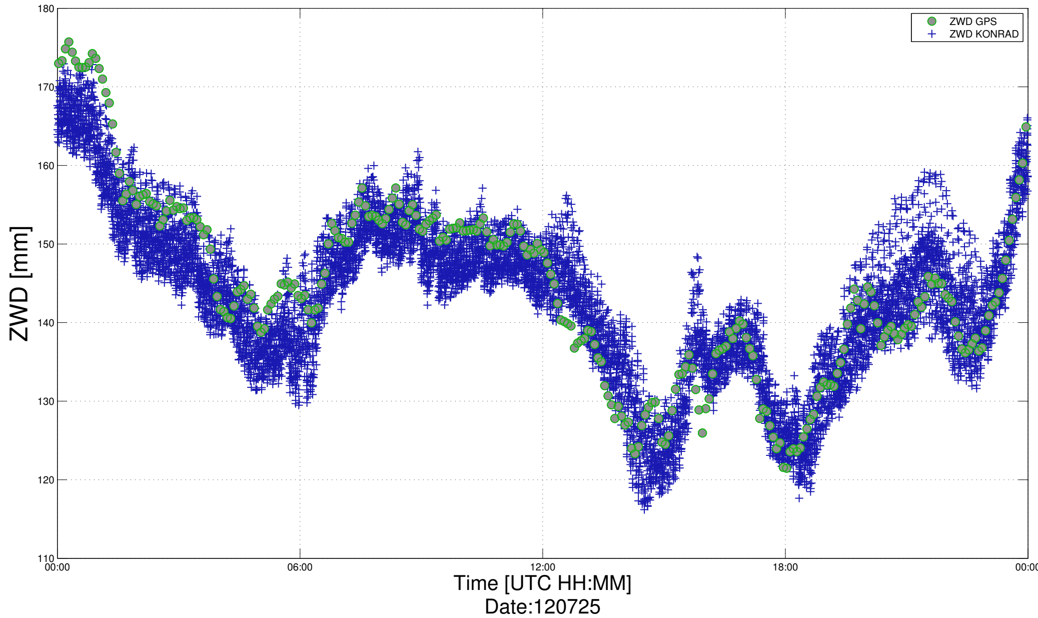

(a)

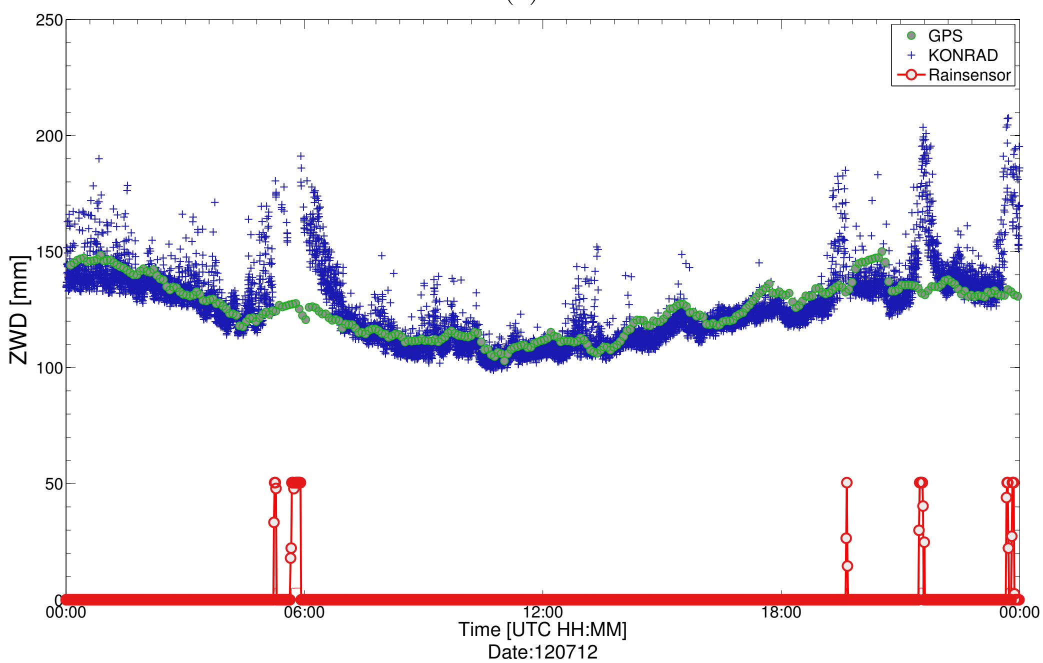

(b)

Figure 2: The ZWD from the Konrad WVR and GPS measurements in a) a clear day : July 12, 2012 and in b) a day with rain showers: July 25, 2012.

2. Experiments

2.1. Weather conditions July 26, 2012

The weather conditions during the first three experiments was sunny and clear with a ground temperature of 17 °C to 19 °C, a relative humidity of 74 % − 78 % and air pressure varying from 1015 hPa to 1017 hPa. The wind speed during the measurements never exceeded 4 m/s. The sky brightness temperature measured by the second radiometer show that T_{sky} drops from 40 K at midnight to the lowest value, 15 K, around 13 UT. Figure 3 show the sky brightness temperature measured by Konrad and Figure 4 the ZWD measurements from GPS and Konrad on the experiment day.

Table 1: Case summary July 26, 2012

Case	Description
C1	Reflector sprayed with droplets
C2	Transmission window sprayed with droplets
C3	Transmission window and reflector sprayed with droplets

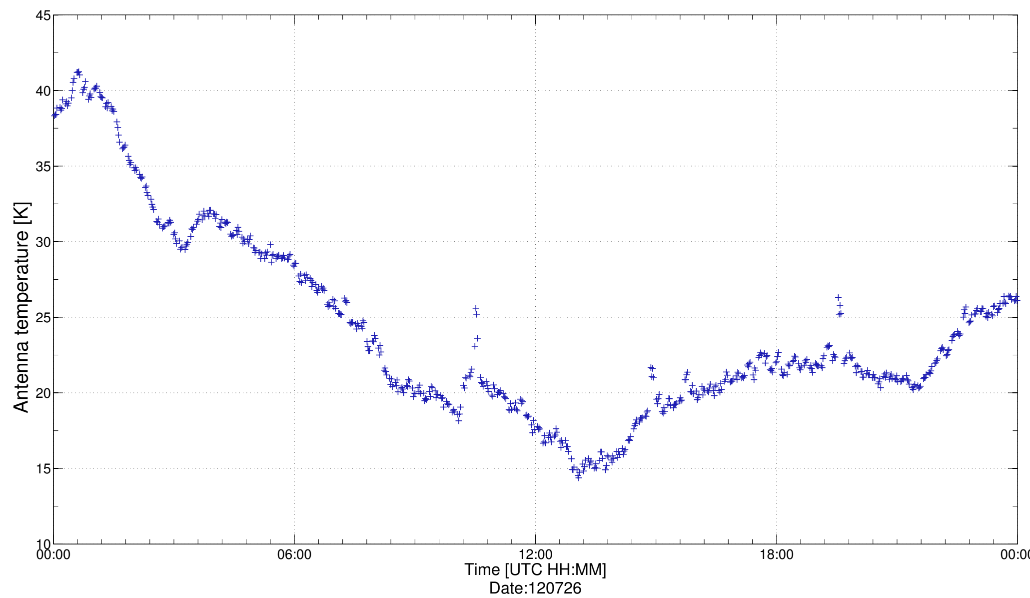

Figure 3: The antenna temperature at 21 GHz on July 26, 2012 measured with the Konrad WVR.

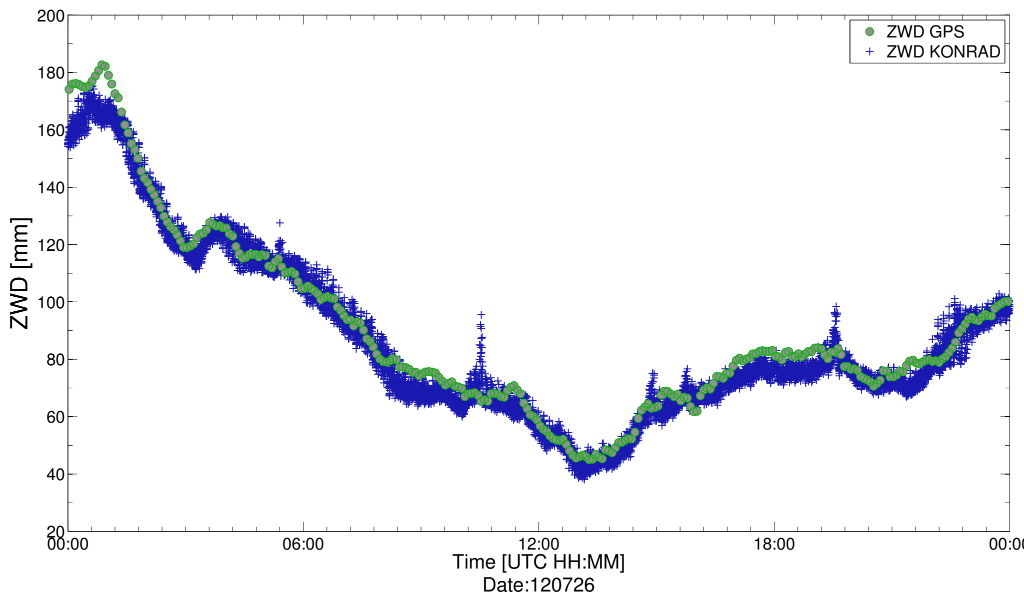

Figure 4: The ZWD on July 26, 2012.

2.2. Case 1: Reflector sprayed with droplets

In Case 1 the reflector was sprayed with droplets. These droplets are, as seen in Figure 5, not uniformly distributed over the reflector area. The area where the radiation is reflected into the transmission window is a part of the reflector area which, due to the geometry, has the shape of a deformed ellipsoid with its center approximately 10 cm to the right of the center of the reflector. In Figure 5 it can be seen that this area has less water drops than the surrounding area. The measurement of the brightness temperature and the ZWD are plotted in Figure 6a and Figure 6b, respectively. The result from the experiment is summarized in Table 2.

Figure 5: The reflector at the start of Case 1.

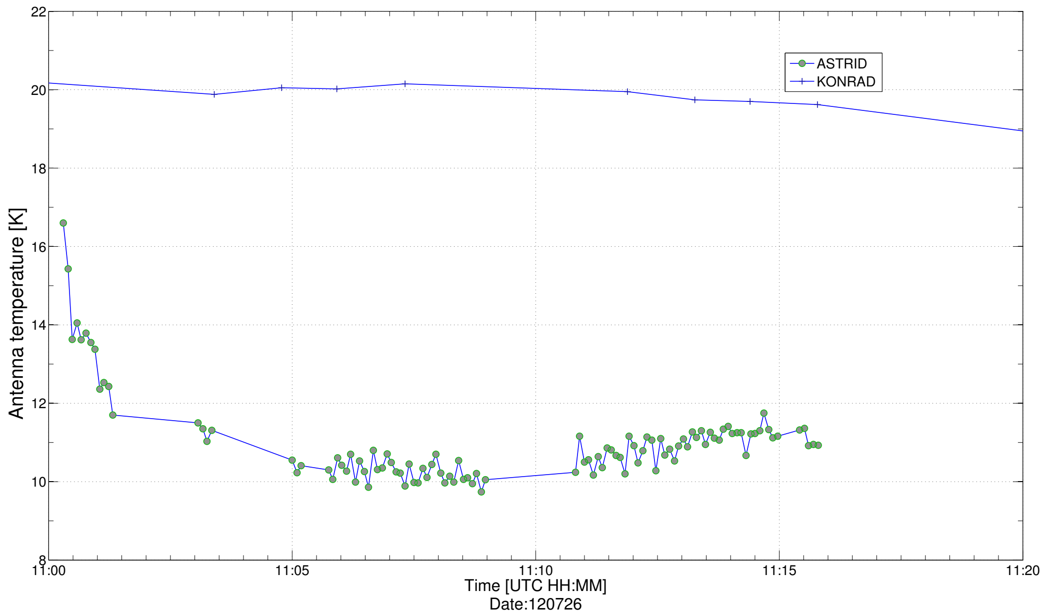

(a)

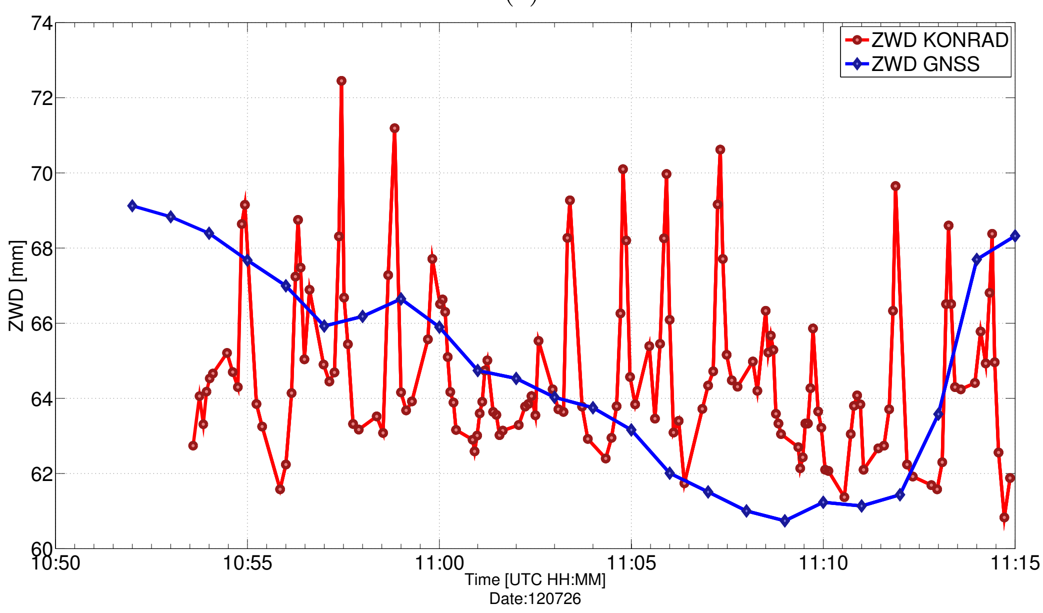

(b)

Figure 6: a) The antenna temperature from Astrid and Konrad b) the ZWD, both during Case 1.

Table 2: Case 1

Case	1
Start – end time [UT]	11:01:00 – 11:16:00
T_A^{Start}[K]	17.8
T_A^{End}[K]	13.5
$T_{A90\%}@time$[K@HH : mm : SS]	16.02@11:03:15
$T_{A10\%}@time$[K@HH : mm : SS]	12.15@11:15:31
τ	12 min 16 s
Δ ZWD [mm]	-2

2.3. Case 2: Transmission window sprayed with drops

In Case 2 the transmission window was sprayed with drops while the reflector was dry (see Figure 7). Figure 8a depicts the brightness temperature and Figure 8b the ZWD measured during the experiment. Table 3 summarize the results from Case 2.

Figure 7: The transmission window at the start of Case 2.

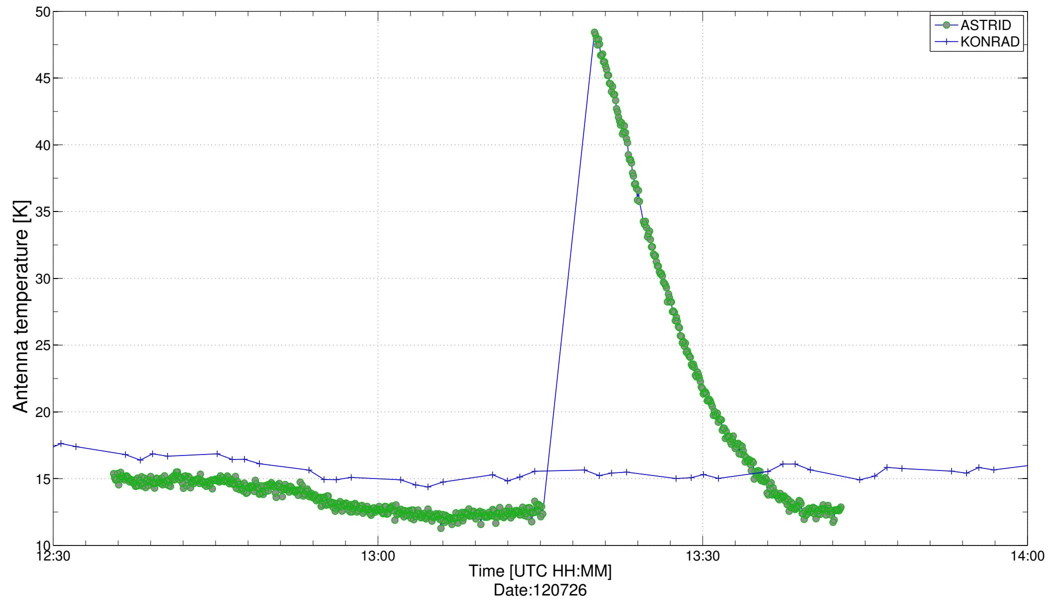

(a)

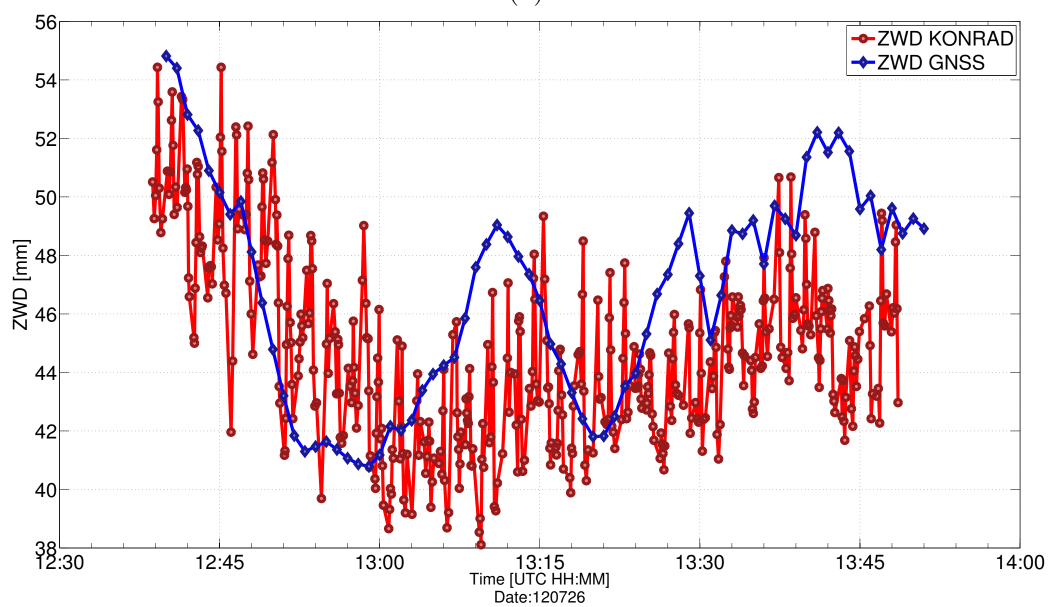

(b)

Figure 8: a) The antenna temperature from Astrid and Konrad b) the ZWD, both during Case 2.

Table 3: Case 2

Case	2
Start – end time [UT]	13:20:45 - 13:47:50
T_A^{Start}[K]	42.6
T_A^{End}[K]	8.8
$T_{A90\%}@time[\mathrm{K@HH:mm:SS}]$	38.37 @ 13:22:08
$T_{A10\%}@time[\mathrm{K@HH:mm:SS}]$	9.64 @ 13:36:47
τ	14 min 39 s
Δ ZWD [mm]	0

2.4. Case 3: Transmission window and reflector sprayed with droplets

In Case 3 the transmission window and the reflector were sprayed with droplets (see Figure 9). The reflector was, as discussed in Case 1, not uniformly sprayed with drops and the amount of water in the area where the radiation reflects are not measured. Therefore, Case 1 and Case 3 are not directly comparable. Table 4 summarizes the results from Case 3.

Figure 9: The transmission window at the start of Case 3.

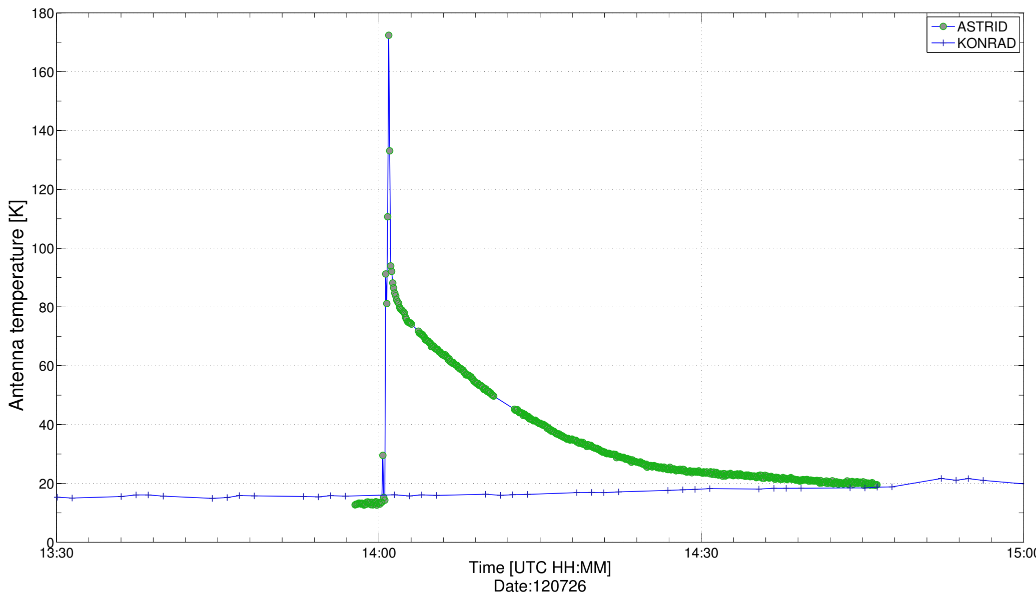

(a)

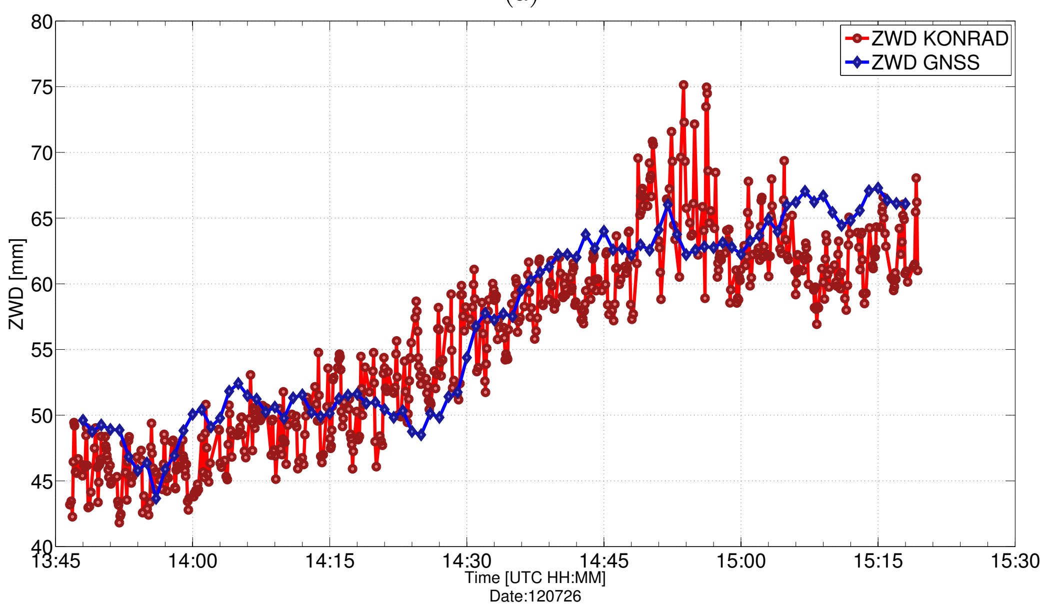

(b)

Figure 10: a) The antenna temperature from Astrid and Konrad b) the ZWD, both during Case 3.

Table 4: Case 3

Case	3
Start – End time [UT]	14:01:17 - 14:53:33
T_A^{Start}[K]	84.8
T_A^{End}[K]	12.2
$T_{A90\%}@time$[K@HH : mm : SS]	76.32 @ 14:01:56
$T_{A10\%}@time$[K@HH : mm : SS]	13.42 @ 14:50:36
τ	48 min 40 s
Δ ZWD [mm]	14

2.5. Weather conditions August 31, 2012

The weather conditions during the fourth experiment was partly cloudy with a ground temperature at 17 °C, air humidity of 76 % and air pressure at 1011 hPa. The sky brightness temperature measured by the second radiometer show a variation of about 1 K during the experiment.

Table 5: Case summary August 31, 2012

Case	Description
C4	Droplets placed on the reflector

2.6. Case 4: Droplets placed on the reflector

In Case 4 droplets were carefully placed on the reflector in a rectangular grid about 15 drops wide and 13 drops high (see Figure 11). They were placed in front of the 21 GHz transmission window. Figure 12 depicts the brightness temperature from Astrid and Konrad together with pictures of the reflector at the indicated time epochs.

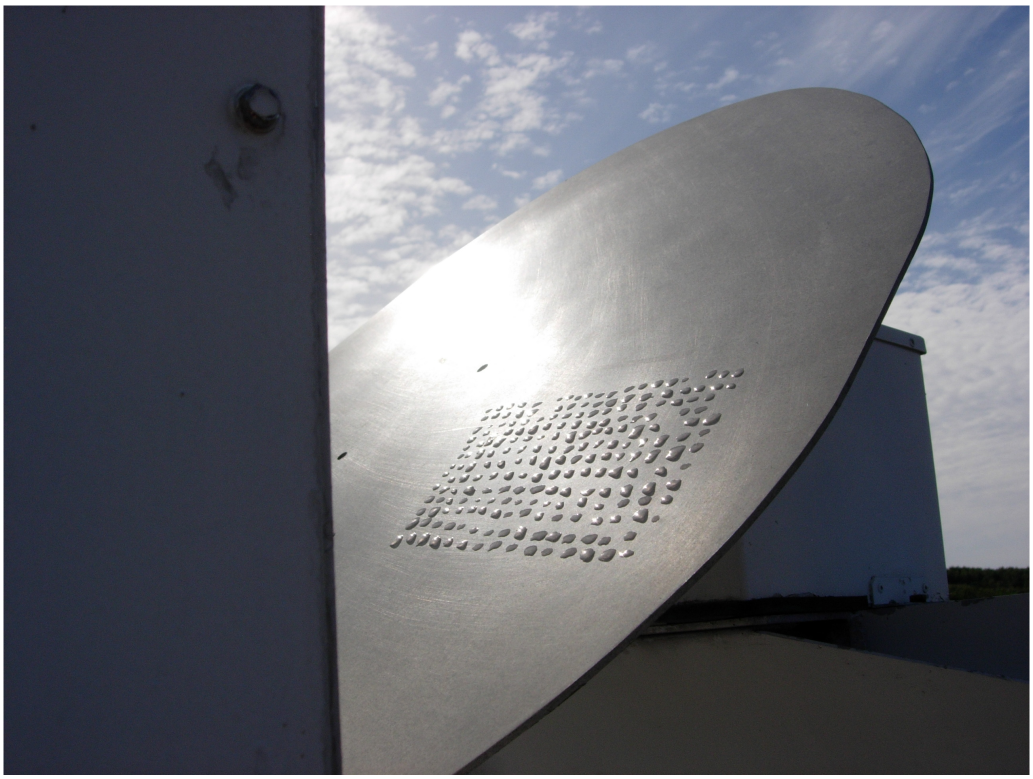

Figure 11: The reflector surface at the start of Case 4.

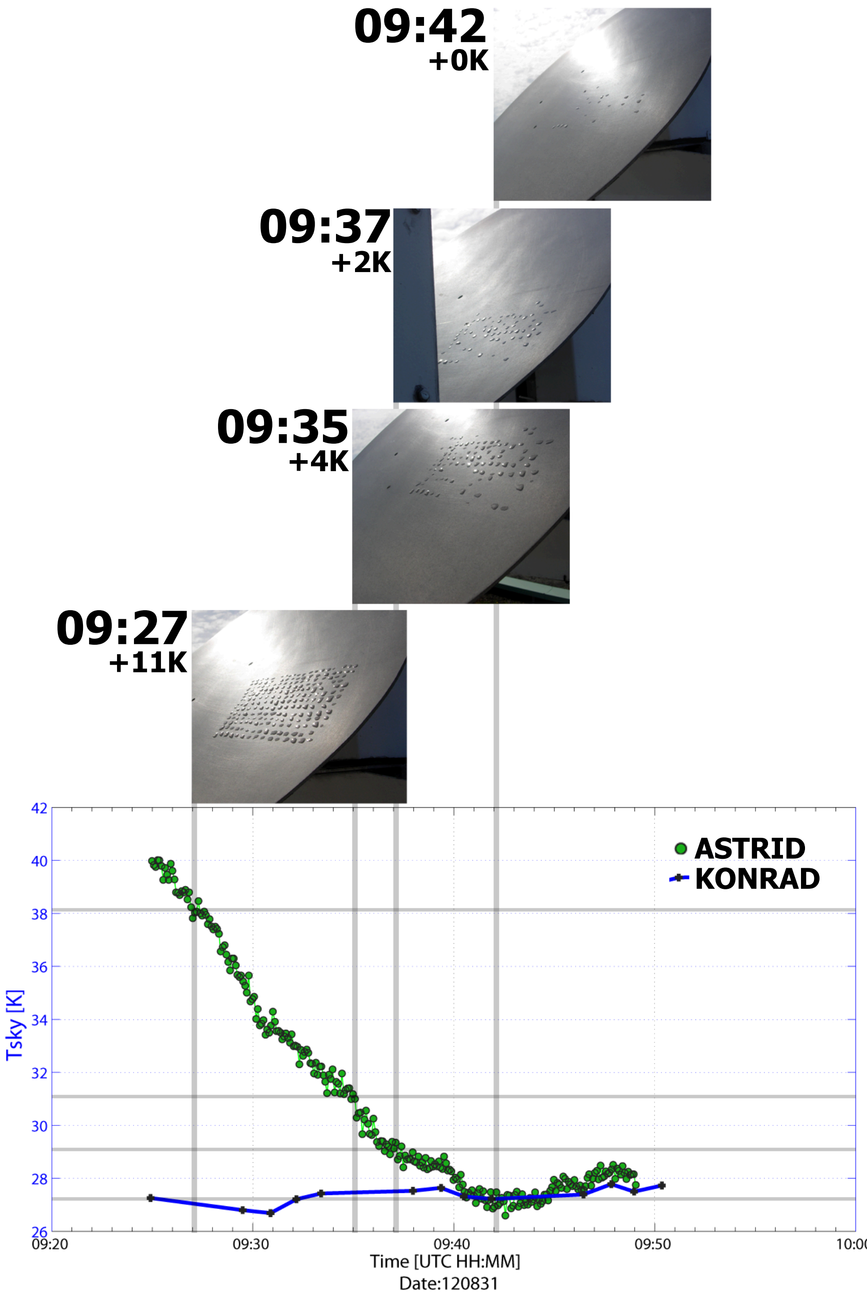

Figure 12: The antenna temperature from Astrid and Konrad together with pictures of the droplets on the reflector.

Table 6: Case 4

Case	4
Start – End time [UT]	09:25:00 - 09:49:00
T_A^{Start}[K]	40.0
T_A^{End}[K]	28.0
$T_{A90\%}@time$[K@HH : mm : SS]	38.7 @ 09:26:00
$T_{A10\%}@time$[K@HH : mm : SS]	28.3 @ 09:40:00
τ	14 min 00 s
Δ ZWD [mm]	–

3. Discussion of results

The antenna temperature, T_A, from Astrid and a reference time series from Konrad are plotted for all four cases. The added water droplets evaporate quickly and the time dependence of the evaporation follow the expected second order polynomial due to the geometry of the reflector and transmission window. During the measurements the reference temperature from Konrad was stable and varied at most about 2 K. The ZWD from Konrad and GNSS during the measurement were also stable and did not vary more than 20 mm.
In Case 1 the reflector was sprayed with droplets which gave a 4 K increase in T_A. The temperature is 10 K under the reference at 21 K which was found to be due to a problem with the absolute calibration during the measurements. That is, however, of secondary importance since we are measuring the temperature difference.
In Case 2, where the transmission window was sprayed, a much bigger impact on the temperature was seen which is explained by a higher density of water since droplets stick easier on the plastic transmission window than on the metallic reflector, and by the fact that the reflection losses are bigger since almost all reflected radiation reflects away from the receiver.
Case 3 gave more than double the increase in T_A when one would expect the sum of the previous two cases. The explanation is probably that a higher density of droplets was placed both on the reflector and especially on the transmission window.
In Case 4 droplets were placed in a grid on the reflector. The effect from these droplets was much larger than in Case 1 which also could be explained by a higher density of water on the part of the reflector directly in front of the transmission window.

Table 7: Summary

Case	Description	Excess T (K)	Time constant τ
1	Reflector sprayed with droplets	4	12 min 16 s
2	Transmission window sprayed with droplets	34	14 min 39 s
3	Transmission window and reflector sprayed with droplets	72	48 min 40 s
4	Droplets placed on the reflector	13	14 min 00 s

4. Conclusion

All measurements were made in the zenith direction. In a normal setup the reflector would move and therefore accumulated rain is not expected to stay as long on the reflector in such a case. During this experiment the metallic reflector was heated by the sun. We found that water droplets easier stick and evaporate slower on the transmission window than on the reflector under these conditions. The time constant in all cases is expected to be longer in rainy conditions when the air humidity is higher and both the air and reflector temperature are lower. In a heavy rain a considerate amount of droplets stick to the transmission window and the time constant is expected to reach almost 1 h.

References

Elgered, G., and P.O.J. Jarlemark, Ground-Based Microwave Radiometry and Long-Term Observations of Atmospheric Water Vapor, *Radio Sci.*, **33**, 707–717, 1998.

Jacobson, M.D., Hogg D.C., & Snider J.B., Wet Reflectors in Millimeter-Wave Radiometry-Experiment and Theory *IEEE Trans. Geosci. Rem. Sens.* **GE-24**, 5. pp. 784-791, September 1986.

Stoew, B., C. Rieck, and G. Elgered, First results from a new dual-channel water vapor radiometer, *Proc. of the 14th Working Meeting on European VLBI for Geodesy and Astrometry*, Castel San Pietro Terme, 8–9 September, 2000, edited by P. Tomasi, F. Mantovani, and M. Perez Torres, pp. 79–82, 2000.